LETTER

doi:10.1038/nature10921

IFITM3 restricts the morbidity and mortality associated with influenza

Aaron R. Everitt[1], Simon Clare[1], Thomas Pertel[2], Sinu P. John[2], Rachael S. Wash[1], Sarah E. Smith[1], Christopher R. Chin[2], Eric M. Feeley[2], Jennifer S. Sims[2], David J. Adams[1], Helen M. Wise[3], Leanne Kane[1], David Goulding[1], Paul Digard[3], Verneri Anttila[1], J. Kenneth Baillie[4,5], Tim S. Walsh[5], David A. Hume[4], Aarno Palotie[1], Yali Xue[1], Vincenza Colonna[1,6], Chris Tyler-Smith[1], Jake Dunning[7], Stephen B. Gordon[8], The GenISIS Investigators*, The MOSAIC Investigators*, Rosalind L. Smyth[9], Peter J. Openshaw[7], Gordon Dougan[1], Abraham L. Brass[2,10] & Paul Kellam[1,11]

The 2009 H1N1 influenza pandemic showed the speed with which a novel respiratory virus can spread and the ability of a generally mild infection to induce severe morbidity and mortality in a subset of the population. Recent *in vitro* studies show that the interferon-inducible transmembrane (IFITM) protein family members potently restrict the replication of multiple pathogenic viruses[1–7]. Both the magnitude and breadth of the IFITM proteins' *in vitro* effects suggest that they are critical for intrinsic resistance to such viruses, including influenza viruses. Using a knockout mouse model[8], we now test this hypothesis directly and find that IFITM3 is essential for defending the host against influenza A virus *in vivo*. Mice lacking *Ifitm3* display fulminant viral pneumonia when challenged with a normally low-pathogenicity influenza virus, mirroring the destruction inflicted by the highly pathogenic 1918 'Spanish' influenza[9,10]. Similar increased viral replication is seen *in vitro*, with protection rescued by the re-introduction of *Ifitm3*. To test the role of IFITM3 in human influenza virus infection, we assessed the *IFITM3* alleles of individuals hospitalized with seasonal or pandemic influenza H1N1/09 viruses. We find that a statistically significant number of hospitalized subjects show enrichment for a minor *IFITM3* allele (SNP rs12252-C) that alters a splice acceptor site, and functional assays show the minor CC genotype IFITM3 has reduced influenza virus restriction *in vitro*. Together these data reveal that the action of a single intrinsic immune effector, IFITM3, profoundly alters the course of influenza virus infection in mouse and humans.

IFITM3 was identified in a functional genomic screen as mediating resistance to influenza A virus, dengue virus and West Nile virus infection *in vitro*[1]. However, the role of the IFITM proteins in antiviral immunity *in vivo* is unknown. Therefore, we infected mice that are homozygous for a disruptive insertion in exon 1 of the *Ifitm3* gene that abolishes its expression[8] (*Ifitm3*$^{-/-}$) with a low-pathogenicity murine-adapted H3N2 influenza A virus (A/X-31). Low-pathogenicity strains of influenza do not normally cause extensive viral replication throughout the lungs, or cause the cytokine dysregulation and death typically seen after infection with highly pathogenic viral strains[9], at the doses used (Fig. 1a). However, low-pathogenicity-infected *Ifitm3*$^{-/-}$ mice became moribund, losing >25% of their original body weight and showing severe signs of clinical illness (rapid breathing, piloerection) 6 days after infection. In comparison, wild-type littermates shed <20% of their original body weight, before fully recovering (Fig. 1a, b). There was little difference in virus replication in the lungs during the first 48 h

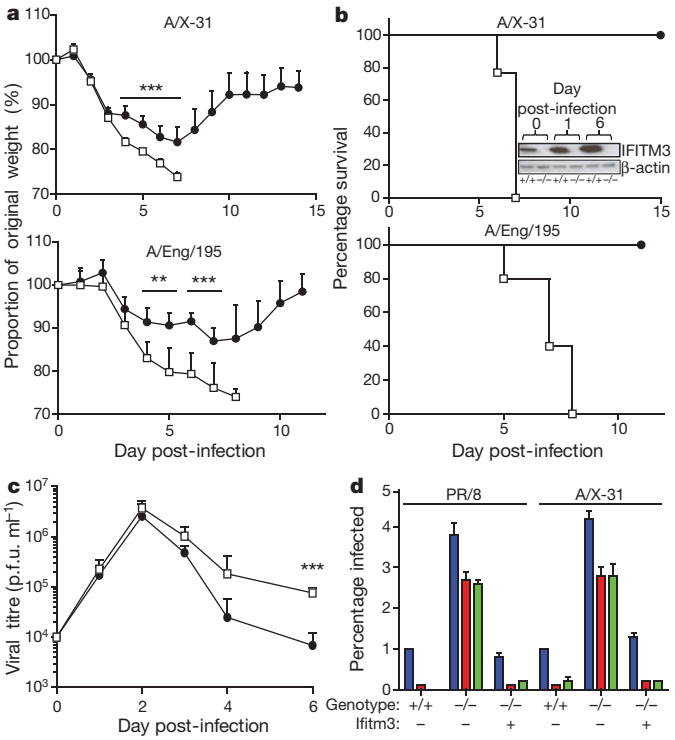

Figure 1 | Influenza A virus replicates to higher levels in *Ifitm3*$^{-/-}$ mice. **a**, **b**, Change in body mass (**a**) and survival (**b**) of wild-type (filled circles) and *Ifitm3*$^{-/-}$ (open squares) mice following intranasal inoculation with A/X-31 and pandemic H1N1/09 Eng/195 influenza ($n > 5$). **b**, Absence of Ifitm3 expression was verified in the *Ifitm3*$^{-/-}$ mice at all time points, but was seen to increase in wild-type mice. **c**, A/X-31 viral load in the lungs of mice ($n > 4$) was calculated over the course of infection by plaque assay. p.f.u., plaque-forming units. *Ifitm3*$^{-/-}$ murine embryonic fibroblasts ($n = 3$ per condition) stably expressing *Ifitm3* (+), or the empty vector (−) were left untreated (blue), or incubated with IFN-α (red) or IFN-γ (green), then challenged with either A/X-31 or PR/8 influenza. **d**, Twelve hours after infection, the cells were assessed for either haemagglutinin expression (PR/8), or nucleoprotein expression (A/X-31) IFITM3 expression was determined to be present (+) or absent (−) by western blotting (Supplementary Fig. 2). Results show means ± s.d. Statistical significance was assessed by Student's *t*-test (**$P < 0.01$; ***$P < 0.001$).

[1]Wellcome Trust Sanger Institute, Wellcome Trust Genome Campus, Hinxton CB10 1SA, UK. [2]Ragon Institute of Massachusetts General Hospital, Massachusetts Institute of Technology, and Harvard University, Charlestown, Massachusetts 02129, USA. [3]Divison of Virology, Department of Pathology, University of Cambridge, Tennis Court Road, Cambridge CB2 1QP, UK. [4]Division of Genetics and Genomics, The Roslin Institute, University of Edinburgh, Roslin EH25 9RG, UK. [5]Department of Critical Care Medicine, University of Edinburgh, Edinburgh EH16 4TJ, UK. [6]Institute of Genetics and Biophysics "A. Buzzati-Traverso", National Research Council (CNR), Naples, Italy. [7]Centre for Respiratory Infection, National Heart and Lung Institute, St Mary's Campus, Imperial College London, W2 1PG, UK. [8]Liverpool School of Tropical Medicine, Pembroke Place, Liverpool L3 5QA, UK. [9]Institute of Translational Medicine, University of Liverpool, Alder Hey Children's Hospital, Liverpool L12 2AP, UK. [10]Gastrointestinal Unit, Massachusetts General Hospital, Boston, Massachusetts 02117, USA. [11]UCL/MRC Centre for Medical Molecular Virology, Department of Infection, University College London, Cleveland Street, London W1T 4JF, UK.

*Lists of participants and their affiliations appear at the end of the paper.

of infection. However, virus persisted and was not cleared as quickly in *Ifitm3*$^{-/-}$ mice, whose lungs contained tenfold higher levels of replicating virus than the wild-type mice at 6 days post-infection (Fig. 1c). No viral RNA was detected in the heart, brain or spleen of infected wild-type or *Ifitm3*$^{-/-}$ mice over the course of infection, revealing that systemic viraemia was not occurring. Full-genome sequencing of virus removed from the lungs of wild-type and *Ifitm3*$^{-/-}$ mice showed no genetic variation. We demonstrated that IFITM3 protein expression after influenza infection was absent in *Ifitm3*$^{-/-}$ mice but increased substantially in wild-type controls (Fig. 1b and Supplementary Fig. 1). Infection of wild-type and *Ifitm3*$^{-/-}$ mice with a human isolate of pandemic influenza A H1N1 (pH1N1/09) resulted in the same severe pathogenicity phenotype in the *Ifitm3*$^{-/-}$ mice (Fig. 1a, b). Mouse embryonic fibroblast (MEF) lines generated from multiple matched littermates demonstrated that *Ifitm3*$^{-/-}$ cells are infected more readily *in vitro*, and lack much of the protective effects of interferon (IFN). Importantly, the stable restoration of IFITM3 conferred wild-type levels of restriction against either the X-31 strain, or the more pathogenic Puerto Rico/8/34 (PR/8) influenza strain (Fig. 1d and Supplementary Fig. 2). In addition to the role of IFITM3 in restriction of high-pathogenicity H5N1 avian influenza[7], we also show that it limits infection by recent human influenza A virus isolates and influenza B virus (Supplementary Fig. 3). Therefore, enhanced pathogenesis to diverse influenza viruses is attributable to loss of *Ifitm3* expression and consequential changes in immune defence of the lungs.

Examination of lung pathology showed fulminant viral pneumonia with substantial damage and severe inflammation in the infected *Ifitm3*$^{-/-}$ mice. Lung pathology was characterized by extensive oedema and red blood cell extravasation, as well as pneumonia, haemorrhagic pleural effusion and multiple, large lesions on all lung lobes (Fig. 2a, b and Supplementary Fig. 4). We note that this pathology is similar to that produced by infection of mice and primates with 1918 H1N1 virus[9–11]. Given the higher viral load in *Ifitm3*$^{-/-}$ mice and increased replication of influenza A virus in *Ifitm3*-deleted cells *in vitro* (Fig. 1d), we examined both viral nucleic acid and protein distribution in the lung. Influenza virus infection penetrated deeper into the lung tissue in *Ifitm3*$^{-/-}$ compared to wild-type mice whose infection was primarily restricted to the bronchioles, with minimal alveolar infection. Influenza virus was detected throughout the entire lung in *Ifitm3*$^{-/-}$ sections, spreading extensively in both bronchioles and alveoli (Fig. 2c). Histopathology showed marked infiltration of cells and debris into the bronchoalveolar space of *Ifitm3*$^{-/-}$ mice (Fig. 2b and Supplementary Fig. 4b). The extent and mechanism of cell damage was investigated by TdT-mediated dUTP nick end labelling (TUNEL) assay, showing widespread cellular apoptosis occurring 6 days post-infection in *Ifitm3*$^{-/-}$ mice, whereas apoptosis in wild-type lungs was very limited (Supplementary Fig. 4c). Together, the *Ifitm3*$^{-/-}$ mouse pathology is consistent with infection by high-pathogenicity strains of influenza A virus, where widespread apoptosis occurs by day 6 post-infection, whereas lungs from low-pathogenicity infections were similar to those of wild-type mice, displaying minimal damage[9,12,13].

Analysis of cell populations resident in the lung tissue on day 6 post-infection showed that *Ifitm3*$^{-/-}$ mice had significantly reduced proportions of CD4$^+$ ($P = 0.004$) and CD8$^+$ T cells ($P = 0.02$) and natural killer (NK) cells ($P = 0.0001$), but an elevated proportion of neutrophils ($P = 0.007$) (Fig. 3a). Despite the extensive cellular infiltration (Supplementary Figs 4b, 5a), the absolute numbers of CD4$^+$ T-lymphocytes in the lungs of the *Ifitm3*$^{-/-}$ mice were also lower and neutrophils increased compared to wild-type mice (Supplementary Fig. 6). The peripheral blood of infected *Ifitm3*$^{-/-}$ mice showed leukopenia (Supplementary Fig. 5c). Blood differential cell counts indicated marked depletion of lymphocytes on day 2 post-infection in the *Ifitm3*$^{-/-}$ mice ($P = 0.04$) (Fig. 3b), reflecting changes observed previously in high-pathogenicity (but not low-pathogenicity) influenza infections in both humans and animal models[9,12,14,15]. Heightened cytokine and chemokine levels are also hallmarks of severe influenza infection, having been observed in both human and animal models[9,16]. We observed exaggerated pro-inflammatory responses in the lungs of *Ifitm3*$^{-/-}$ mice with levels of TNF-α, IL-6, G-CSF and MCP-1 showing the most marked increase (Fig. 3c and Supplementary Fig. 7). This is indicative of the extent of viral spread within the lungs, as TNF-α and IL-6 are released from cells upon infection[17]. Consistent with the immunopathology data above, these changes are comparable in level to those seen with non-H5N1 high-pathogenicity influenza infections[9]. Neutrophil chemotaxis, together with elevated proinflammatory cytokine secretion, has previously been reported as one of the primary causes of acute lung injury[18].

To investigate further the extensive damage observed with low-pathogenicity influenza A virus infection in the absence of IFITM3, we infected both wild-type and *Ifitm3*$^{-/-}$ mice with a PR/8 influenza strain deficient for the multi-functional *NS1* gene (delNS1)[19,20]. NS1 is the primary influenza virus interferon antagonist, with multiple inhibitory effects on host immune pathways[20,21]. We found that delNS1 virus was attenuated in both wild-type and *Ifitm3*$^{-/-}$ mice, and whereas the isogenic PR/8 strain expressing NS1 showed typical high pathogenicity in all mice tested, lower doses of PR/8 influenza (although lethal in both genotypes of mice) caused accelerated weight loss in *Ifitm3*$^{-/-}$ compared to wild-type mice (Supplementary Fig. 8). As delNS1 influenza A virus retains its pathogenicity in IFN-deficient mice[19], this suggests that *Ifitm3*$^{-/-}$ mice can mount an adequate IFN-mediated anti-viral response without extensive morbidity, and that IFITM3 blocking viral replication occurs before NS1-mediated IFN

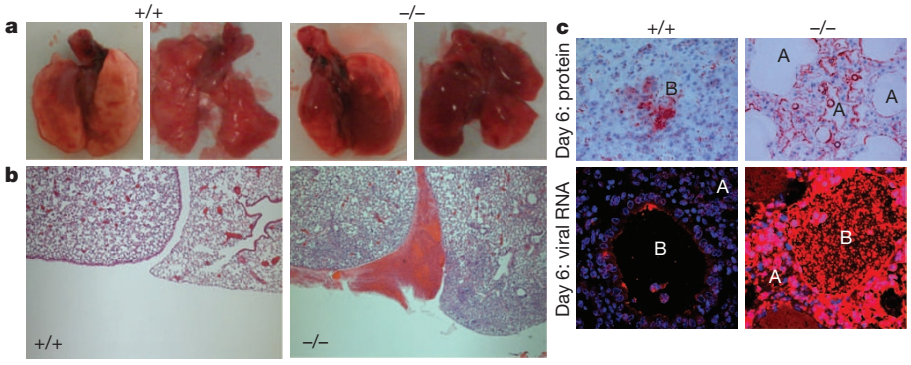

Figure 2 | Pathological examination of infected lungs. **a**, **b**, Wild-type mice showed few visible signs of external damage on lung lobes at day 6 post-infection, whereas *Ifitm3*$^{-/-}$ mice showed several large lesions (**a**, left, ventral view of intact lungs, right, all lobes displayed) resulting from severe oedema and hemorrhagic pleural effusion (**b**), as well as a markedly higher infiltration of cells and proteinaceous debris into the alveoli and bronchioles. **c**, Localization of virus within the lungs on day 6 indicated that virus penetrated deeper and more extensively into the lung tissue in the *Ifitm3*$^{-/-}$ mice, as determined by immunohistochemistry for total influenza protein and detection of virus nucleic acid (virus, red; cell nuclei, blue; A, alveolus; B, bronchiole). Original magnifications were ×5 (**b**) and ×20 (**c**).

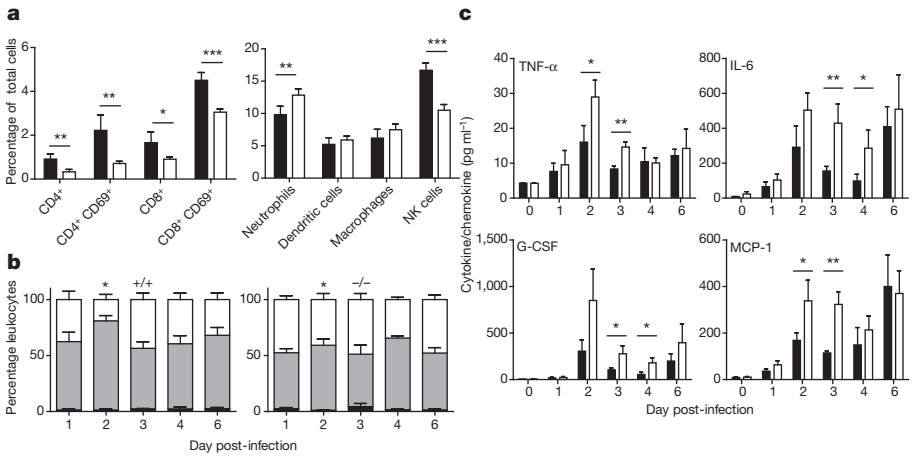

Figure 3 | Altered leukocyte and cytokine response to influenza A infection in *Ifitm3*$^{-/-}$ mice. **a**, Cytometric analysis of proportional resident cell populations in the lungs of mice (+/+, black; −/−, white) showed evidence of lymphopenia in *Ifitm3*$^{-/-}$ mice 6 days post-infection. **b**, Systemic lymphopenia was confirmed through differential analysis of peripheral blood cell counts, which showed a significant depletion of lymphocytes on day 2 post-infection of *Ifitm3*$^{-/-}$ mice (monocytes, black; lymphocytes, grey; polymorphonuclear leukocytes, white). NK, natural killer. **c**, Levels of pro-inflammatory cytokines were also recorded as being elevated in *Ifitm3*$^{-/-}$ lungs over the course of infection (+/+, black; −/−, white). Results show means ± s.d., $n = 5$. Statistical significance was assessed by Student's *t*-test ($*P < 0.05$, $**P < 0.01$, $***P < 0.001$).

antagonism[7]. Therefore, unchecked lung viral replication and an enhanced inflammatory response accounts for the profoundly deleterious effects of viral infection in *Ifitm3*$^{-/-}$ mice.

The human *IFITM3* gene has two exons and is predicted to encode two splice variants that differ by the presence or absence of the first amino-terminal 21 amino acids (Fig. 4a). Currently, 13 non-synonymous, 13 synonymous, one in-frame stop and one splice site acceptor-altering single nucleotide polymorphisms (SNPs) have been reported in the translated *IFITM3* sequence (Supplementary Table 1). Using tests sensitive to recent positive selection, we can find evidence for positive selection on the *IFITM3* locus in human populations acting over the last tens of thousands of years in Africa (Fig. 4b, c). We therefore

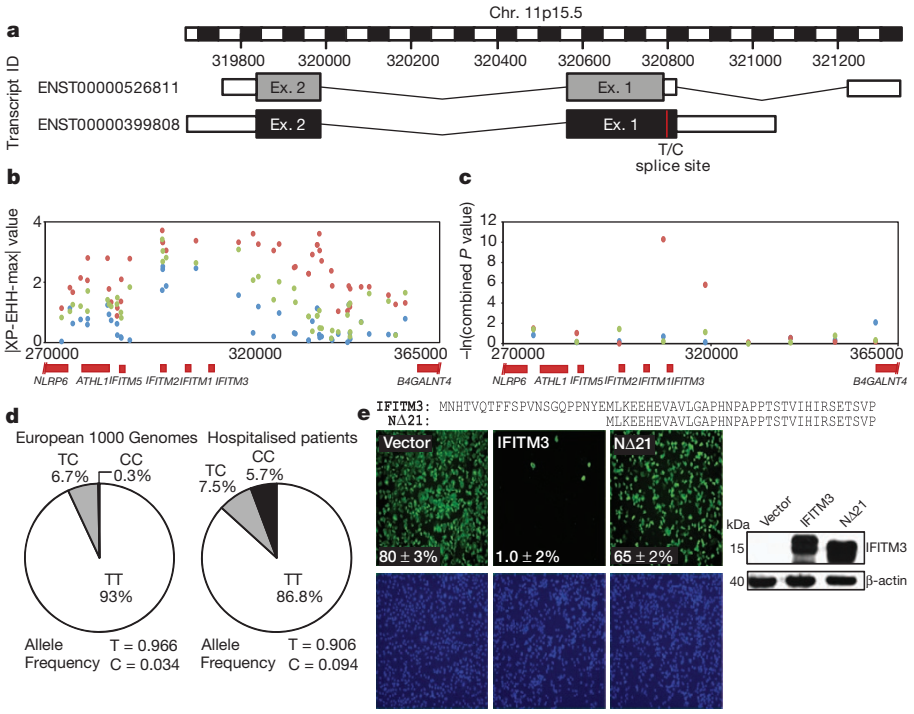

Figure 4 | Single nucleotide polymorphisms of the human *IFITM3* gene. **a**, Multiple single-nucleotide polymorphisms have been identified within the coding region of the human *IFITM3* gene. One such SNP, rs12252 (red), encodes a splice acceptor site altering T/C substitution mutation and may be associated with a truncated protein with an N-terminal 21 amino acid deletion. Therefore two transcripts are predicted to be expressed from the *IFITM3* gene. **b**, **c**, Positive selection analysis using a haplotype-based test, the cross population extended haplotype homozygosity test, maximum value (|XP-EHH-max|, **b**), where data points above 2.7 in the YRI (Africa) (red), 3.9 in the CEU (Europe) (blue) and 5.0 in the CHB+JPT (China and Japan) (green) populations are in the top 1% of values, and using a combination of three allele frequency spectrum-based test statistics (**c**), namely the composite likelihood ratio (CLR)[23–25] on 10-kb windows along chromosome 11 encompassing the *IFITM3* locus. Evidence for positive selection is seen only in the YRI. **d**, Mutations recorded through sequencing of patients hospitalized with influenza virus during the H1N1/09 pandemic showed an overrepresentation of individuals with the C allele at SNP rs12252, relative to matched Europeans. **e**, A549 cells transduced to express either full-length (IFITM3) or truncated (NΔ21) IFITM3 (cell nuclei, blue; virus, green; ×4 magnification) show a reduction in viral restriction when the N-terminal 21 amino acids of IFITM3 are removed, relative to vector controls (Vector). Alignment of the N termini of full-length (IFITM3, top) and truncated IFITM3 (NΔ21, bottom). Values represent the mean of the percentage of infected cells ± s.d. ($n = 3$).

sequenced 1.8 kilobases of the *IFITM3* locus encompassing the exons, intron and untranslated regions from 53 individuals who required admission to hospital as a result of pandemic H1N1/09 or seasonal influenza virus infection in 2009–2010. Of these, 86.8% of patients carried majority alleles for all 28 SNPs in the coding sequence of the gene, but 13.2% possessed known variants. In particular, we discovered over-representation in cases of the synonymous SNP rs12252, wherein the majority T allele is substituted for a minority C allele, which alters the first splice acceptor site and may be associated with the *IFITM3* splice variant (ENST00000526811), which encodes an IFITM3 protein lacking the first 21 amino acids due to the use of an alternative start codon.

The allele frequencies for SNP rs12252 vary in different human populations (Supplementary Table 2). The ancestral (C) allele, reported in chimpanzees, is rare in sub-Saharan African and European populations (derived allele frequency (DAF) 0.093 and 0.026–0.036, respectively), but more frequent in other populations (Supplementary Table 2). SNP rs12252 is notable for its high level of differentiation between Europeans and East Asians, although the fixation index (F_{ST}, a measure of population differentiation) does not reach statistical significance. The genotypes associated with rs12252 in Caucasians hospitalized following influenza infection differ significantly from ethnically matched Europeans in 1000 Genomes sequence data and from genotypes imputed against the June 2011 release of the 1000 Genomes phased haplotypes from the UK, Netherlands and Germany (Wellcome Trust Case Control Consortium 1 (WTCCC1, UK): $P = 0.00006$, Netherlands: $P = 0.00001$, Germany: $P = 0.00007$; Fisher's exact test). Patients' genotypes also depart from Hardy–Weinberg equilibrium ($P = 0.003$), showing an excess of C alleles in this population (Fig. 4d). Principal components analysis of over 100,000 autosomal SNPs showed no evidence of hidden population structure differences between WTCCC controls and a subset of the hospitalised individuals from this study (Supplementary Fig. 9a, b).

To test the functional significance of the IFITM3 rs12252 polymorphism *in vitro*, we confirmed the genotypes of HapMap lymphoblastoid cell lines (LCLs) homozygous for either the majority (TT) or minority (CC) variant IFITM3 alleles (Supplementary Fig. 9c). We next challenged the LCLs with influenza A virus and found that the minority (CC) variant was more susceptible to infection, and this vulnerability correlated with lower levels of IFITM3 protein expression compared to the majority (TT) variant cells (Supplementary Fig. 10). Although we did not detect the IFITM3 splice variant protein (ENST00000526811) in the CC LCLs, we nonetheless investigated the possible significance of its presence by stably expressing the N-terminally truncated (NΔ21) and wild-type proteins to equivalent levels in human A549 lung carcinoma cell lines before infection with influenza A virus (A/WSN/1933 (WSN/33)). We found that cells expressing the NΔ21 protein failed to restrict viral replication when compared to wild-type IFITM3 (Fig. 4e), consistent with previous data showing that the amino-terminal 21 amino acids of IFITM3 are required for attenuation of vesicular stomatitis virus replication *in vitro*[4]. Similar results were obtained using other virulent viral strains (A/California/7/2009 (pH1N1), A/Uruguay/716/2007 (H3N2) and B/Brisbane/60/2008) (Supplementary Fig. 3).

We show here that IFITM3 expression acts as an essential barrier to influenza A virus infection *in vivo* and *in vitro*. The fulminant viral pneumonia that occurs in the absence of IFITM3 arises because of uncontrolled virus replication in the lungs, resulting in profound morbidity. In effect, the host's loss of a single immune effector, IFITM3, transforms a mild infection into one with remarkable severity. Similarly, the enrichment of the rs12252 C-allele in those hospitalized with influenza infections, together with the decreased IFITM3 levels and the increased infection of the CC-allele cells *in vitro*, suggests that IFITM3 also plays a pivotal role in defence against human influenza virus infections. This innate resistance factor is all the more important during encounters with a novel pandemic virus, when the host's acquired immune defences are less effective. Indeed, IFITM3-compromised individuals, and in turn populations with a higher percentage of such individuals, may be more vulnerable to the initial establishment and spread of a virus against which they lack adaptive immunity. In light of its ability to curtail the replication of a broad range of pathogenic viruses *in vitro*, these *in vivo* results suggest that IFITM3 may also shape the clinical course of additional viral infections in favour of the host, and may have done so over human evolutionary history.

METHODS SUMMARY

Mouse infection. Wild-type and *Ifitm3*$^{-/-}$ mice[8] (8–10 weeks of age) were intranasally inoculated with 10^4 p.f.u. of A/X-31 (H3N2) influenza, 200 p.f.u. of A/England/195/09 (pH1N1) influenza, or 50–10^3 p.f.u. of A/PR/8/34 (PR/8) or the PR/8 *NS1* gene deletion mutant (delNS1)[20] (H1N1) in 50 µl of sterile PBS. Mouse weight was recorded daily as well as monitoring for signs of illness. Mice exceeding 25% total weight loss were killed in accordance with UK Home Office guidelines. Infected lungs were collected on days 1–6 post-infection and quantified for viral load by plaque assay and RT-qPCR with primers to influenza matrix 1 protein.

Pathology of infected *Ifitm3*$^{-/-}$ mice. 5-µm sections of paraffin-embedded tissue were stained with haematoxylin and eosin and microscopically examined. Apoptosis was assessed by TUNEL using the TACS XL DAB *In Situ* Apoptosis Detection Kit (R&D Systems). Viral RNA was visualized by QuantiGene viewRNA kit (Affymetrix), with a viewRNA probe set designed to the negative stranded vRNA encoding the *NP* gene of A/X-31 (Affymetrix). Lung tissue was embedded in glycol methacrylate (GMA) and viral antigens stained using M149 polyclonal antibody to influenza A, B (Takara). Single cell suspensions from the lung were characterized by flow cytometry for T-lymphocytes $CD4^+$ or $CD8^+$, T-lymphocytes (activated) $CD4^+CD69^+$ or $CD8^+CD69^+$, neutrophils $CD11b^{hi}CD11c^-Ly6g^+$, dendritic cells $CD11c^+CD11b^{lo}Ly6g^{lo}$ MHC class II high, macrophages $CD11b^+CD11c^+F4/80^{hi}$, natural killer cells $NKp46^+CD4^-CD8^-$.

Sequencing and genetics of human *IFITM3*. The 1.8 kb of human *IFITM3* was amplified and sequenced to identify single nucleotide polymorphisms (SNPs). SNP rs12252 was identified and compared to allele and genotype frequencies from 1000 Genomes sequencing data from different populations including 1000 Genomes imputed. SNP rs12252 allele frequencies were determined in the publicly available genotype data sets of WTCCC1 ($n = 2{,}938$) and previously published data sets genotyped from the Netherlands ($n = 8{,}892$) and Germany ($n = 6{,}253$)[22].

Full Methods and any associated references are available in the online version of the paper at www.nature.com/nature.

Received 7 September 2011; accepted 8 February 2012.
Published online 25 March 2012.

1. Brass, A. L. *et al.* The IFITM proteins mediate cellular resistance to influenza A H1N1 virus, West Nile virus, and dengue virus. *Cell* **139,** 1243–1254 (2009).
2. Jiang, D. *et al.* Identification of five interferon-induced cellular proteins that inhibit West Nile virus and dengue virus infections. *J. Virol.* **84,** 8332–8341 (2010).
3. Yount, J. S. *et al.* Palmitoylome profiling reveals S-palmitoylation-dependent antiviral activity of IFITM3. *Nature Chem. Biol.* **6,** 610–614 (2010).
4. Weidner, J. M. *et al.* Interferon-induced cell membrane proteins, IFITM3 and tetherin, inhibit vesicular stomatitis virus infection via distinct mechanisms. *J. Virol.* **84,** 12646–12657 (2010).
5. Huang, I. C. *et al.* Distinct patterns of IFITM-mediated restriction of filoviruses, SARS coronavirus, and influenza A virus. *PLoS Pathog.* **7,** e1001258 (2011).
6. Schoggins, J. W. *et al.* A diverse range of gene products are effectors of the type I interferon antiviral response. *Nature* **472,** 481–485 (2011).
7. Feeley, E. M. *et al.* IFITM3 inhibits influenza A virus infection by preventing cytosolic entry. *PLoS Pathog.* **7,** e1002337 (2011).
8. Lange, U. C. *et al.* Normal germ line establishment in mice carrying a deletion of the *Ifitm/Fragilis* gene family cluster. *Mol. Cell. Biol.* **28,** 4688–4696 (2008).
9. Belser, J. A. *et al.* Pathogenesis of pandemic influenza A (H1N1) and triple-reassortant swine influenza A (H1) viruses in mice. *J. Virol.* **84,** 4194–4203 (2010).
10. Tumpey, T. M. *et al.* Characterization of the reconstructed 1918 Spanish influenza pandemic virus. *Science* **310,** 77–80 (2005).
11. Kobasa, D. *et al.* Aberrant innate immune response in lethal infection of macaques with the 1918 influenza virus. *Nature* **445,** 319–323 (2007).
12. Tumpey, T. M., Lu, X. H., Morken, T., Zaki, S. R. & Katz, J. M. Depletion of lymphocytes and diminished cytokine production in mice infected with a highly virulent influenza A (H5N1) virus isolated from humans. *J. Virol.* **74,** 6105–6116 (2000).
13. Kobasa, D. *et al.* Enhanced virulence of influenza A viruses with the haemagglutinin of the 1918 pandemic virus. *Nature* **431,** 703–707 (2004).
14. Maines, T. R. *et al.* Pathogenesis of emerging avian influenza viruses in mammals and the host innate immune response. *Immunol. Rev.* **225,** 68–84 (2008).
15. Perrone, L. A., Plowden, J. K., Garcia-Sastre, A., Katz, J. M. & Tumpey, T. M. H5N1 and 1918 pandemic influenza virus infection results in early and excessive infiltration of macrophages and neutrophils in the lungs of mice. *PLoS Pathog.* **4,** e1000115 (2008).

16. Fukuyama, S. & Kawaoka, Y. The pathogenesis of influenza virus infections: the contributions of virus and host factors. *Curr. Opin. Immunol.* **23,** 481–486 (2011).
17. Julkunen, I. *et al.* Inflammatory responses in influenza A virus infection. *Vaccine* **19,** S32–S37 (2000).
18. Yum, H. K. *et al.* Involvement of phosphoinositide 3-kinases in neutrophil activation and the development of acute lung injury. *J. Immunol.* **167,** 6601–6608 (2001).
19. García-Sastre, A. *et al.* Influenza A virus lacking the NS1 gene replicates in interferon-deficient systems. *Virology* **252,** 324–330 (1998).
20. Hale, B. G., Randall, R. E., Ortin, J. & Jackson, D. The multifunctional NS1 protein of influenza A viruses. *J. Gen. Virol.* **89,** 2359–2376 (2008).
21. Billharz, R. *et al.* The NS1 protein of the 1918 pandemic influenza virus blocks host interferon and lipid metabolism pathways. *J. Virol.* **83,** 10557–10570 (2009).
22. Anttila, V. *et al.* Genome-wide association study of migraine implicates a common susceptibility variant on 8q22.1. *Nature Genet.* **42,** 869–873 (2011).
23. Tajima, F. Statistical method for testing the neutral mutation hypothesis by DNA polymorphism. *Genetics* **123,** 585–595 (1989).
24. Fay, J. C. & Wu, C.-I. Hitchhiking under positive Darwinian selection. *Genetics* **155,** 1405–1413 (2000).
25. Nielsen, R. *et al.* Genomic scans for selective sweeps using SNP data. *Genome Res.* **15,** 1566–1575 (2005).

Supplementary Information is linked to the online version of the paper at www.nature.com/nature.

Acknowledgements We would like to thank C. Brandt for maintaining mouse colony health and well-being and T. Hussell for provision of A/X-31 virus. We also thank D. Gurdasani and M. Sandhu for statistical analysis of genotype frequencies. We also thank M. Hu and I. Gallego Romero for calculating genome-wide selection statistics. This work was supported by the Wellcome Trust. The MOSAIC work was supported by Imperial's Comprehensive Biomedical Research Centre (cBRC), the Wellcome Trust (090382/Z/09/Z) and Medical Research Council UK. The GenISIS work was supported by the Chief Scientist Office (Scotland). A.L.B. is the recipient of a Charles H. Hood Foundation Child Health Research Award, and is supported by grants from the Phillip T. and Susan M. Ragon Institute Foundation, the Bill and Melinda Gates Foundation's Global Health Program and the National Institute of Allergy and Infectious Diseases (R01AI091786). J.K.B. is supported by a Wellcome Trust Clinical Lectureship (090385/Z/09/Z) through the Edinburgh Clinical Academic Track (ECAT). We acknowledge the assistance of K. Alshafi, E. Bailey, A. Bermingham, M. Berry, C. Bloom, E. Brannigan, S. Bremang, J. Clark, M. C. Cox, M. Cross, L. A. Cumming, S. Dyas, J. England-Smith, J. Enstone, D. Ferreira, N. Goddard, A. Godlee, S. Gormley, M. Guiver, M. O. Hassan-Ibrahim, H. Hill, P. Holloway, K. Hoschler, G. Houghton, F. Hughes, R. R. Israel, A. Jepson, K. D. Jones, W. P. Kelleher, M. Kidd, K. Knox, A. Lackenby, G. Lloyd, H. Longworth, M. Minns, S. Mookerjee, S. Mt-Isa, D. Muir, A. Paras, V. Pascual, L. Rae, S. Rodenhurst, F. Rozakeas, E. Scott, E. Sergi, N. Shah, V. Sutton, J. Vernazza, A. W. Walker, C. Wenden, T. Wotherspoon, A. D. Wright, F. Wurie and the clinical and laboratory staff of the Alder Hey Children's NHS Foundation Trust, Brighton & Sussex University Hospitals NHS Trust, Central Manchester University Hospitals NHS Foundation Trust, Chelsea and Westminster Hospital NHS Foundation Trust, Alder Hey Children's Hospital and Liverpool School of Tropical Medicine, Health Protection Agency Microbiology Services Colindale, Imperial College Healthcare NHS Trust, Liverpool Women's NHS Foundation Trust, Royal Liverpool and Broadgreen University Hospitals NHS Trust, Royal Brompton and Harefield NHS Foundation Trust, The Roslin Institute, Edinburgh, University Hospitals Coventry and Warwickshire NHS Trust. The MOSAIC consortium was supported by several Comprehensive Local Research Networks (CLRNs), the National Institute for Health Research (NIHR), UK, and by the Biomedical Research Centre (BRC) and Unit (BRU) funds. Finally, we thank all patients and their relatives for their generous agreement to inclusion in this study.

Author Contributions A.R.E., G.D., A.L.B. and P.K. designed the study; A.R.E., P.J.O., G.D., A.L.B. and P.K. wrote the manuscript; A.R.E. performed experiments and analysed data; S.C. designed experiments and performed all live animal work; S.E.S. sequenced and analysed the human *Ifitm3* gene; R.S.W., S.E.S., C.R.C., J.S.S., S.P.J., T.P., E.M.F., A.L.B. and L.K. performed experiments; D.J.A. created the genetically-modified *Ifitm3*$^{-/-}$ mouse line; H.M.W. and P.D. made the influenza virus strains and advised on virology; D.G. performed microscopy; Y.X., V.C. and C.T.-S. performed positive selection analyses; V.A. and A.P. performed imputation and analysis of 1000 Genomes data; E.M.F., C.R.C. and A.L.B. performed *in vitro* viewRNA experiments; recruitment and selection of hospitalised individuals infected with influenza virus was co-ordinated by J.K.B., D.A.H. and T.S.W. (GenISIS) and R.L.S., S.B.G., J.D., J.K.B., D.A.H. and P.J.O. (MOSAIC).

Author Information *IFITM3* sequences are deposited in GenBank under the accession numbers JQ610570–JQ610621. Reprints and permissions information is available at www.nature.com/reprints. The authors declare no competing financial interests. Readers are welcome to comment on the online version of this article at www.nature.com/nature. Correspondence and requests for materials should be addressed to P.K. (pk5@sanger.ac.uk) or A.L.B. (abrass@partners.org).

MOSAIC Core Investigators

Benaroya Research Institute, USA D. Chaussabel[1]; **Gartnavel General Hospital, Greater Glasgow, UK** W. E. Adamson[2], W. F. Carman[2]; **Health Protection Agency, UK** C. Thompson[3], M. C. Zambon[3]; **Imperial College London, UK** P. Aylin[4], D. Ashby[4], W. S. Barclay[4], S. J. Brett[4], W. O. Cookson[4], L. N. Drumright[4], J. Dunning[4], R. A. Elderfield[4], L. Garcia-Alvarez[4], B. G. Gazzard[4], M. J. Griffiths[4], M. S. Habibi[4], T. T. Hansel[4], J. A. Herberg[4], A. H. Holmes[4], T. Hussell[4], S. L. Johnston[4], O. M. Kon[4], M. Levin[4], M. F. Moffatt[4], S. Nadel[4], P. J. Openshaw[4], J. O. Warner[4]; **Liverpool School of Tropical Medicine, UK** S. J. Aston[5], S. B. Gordon[5]; **National Institute for Medical Research, UK** A. Hay[6], J. McCauley[6], A. O'Garra[6]; **Roche, Nutley, USA** J. Banchereau[7]; **University College London, UK** A. Hayward[8], P. Kellam[8]; **University of Edinburgh, UK** J. K. Baillie[9], D. A. Hume[9], P. Simmonds[9]; **University of Liverpool, UK** P. S. McNamara[10], M. G. Semple[10], R. L. Smyth[10]; **University of Nottingham, UK** J. S. Nguyen-Van-Tam[11]; **University of Oxford, UK** L.-P. Ho[12], A. J. McMichael[12]; **Wellcome Trust Sanger Institute, UK** P. Kellam[13].

GenISIS Investigators

Critical Care Medicine, University of Edinburgh K. Everingham[14], H. Dawson[14], D. Hope[14], P. Ramsay[14], T. S. Walsh (Local Lead Investigator)[14]; **Generation Scotland, University of Edinburgh Molecular Medicine Centre** A. Campbell[15], S. Kerr[15]; **Intensive Care National Audit & Research Centre, London** D. Harrison[16], K. Rowan[16]; **Intensive Care Unit, Aberdeen Royal Infirmary** J. Addison[17], N. Donald[17], S. Galt[17], D. Noble[17], J. Taylor[17], N. Webster (Local Lead Investigator)[17]; **Intensive Care Unit, Ayr Hospital** I. Taylor (Local Lead Investigator)[18]; **Intensive Care Unit, Borders General Hospital, Melrose** J. Aldridge (Local Lead Investigator)[19], R. Dornan[19], C. Richard[19]; **Intensive Care Unit, Crosshouse Hospital, Kilmarnock** D. Gilmour[20], R. Simmons (Local Lead Investigator)[20], R. White (Local Lead Investigator)[20]; **Intensive Care Unit, Dumfries and Galloway Royal Infirmary** C. Jardine[21], D. Williams (Local Lead Investigator)[21]; **Intensive Care Unit, Glasgow Royal Infirmary** M. Booth (Local Lead Investigator)[22], T. Quasim[22]; **Intensive Care Unit, Hairmyres Hospital, Lanarkshire** V. Watson[23]; **Intensive Care Unit, Inverclyde Royal Hospital, Greenock** P. Henry[24], F. Munro[24]; **Intensive Care Unit, Monklands Hospital, Airdrie** L. Bell[25], J. Ruddy (Local Lead Investigator)[25]; **Intensive Care Unit, Ninewells Hospital, Dundee** S. Cole (Local Lead Investigator)[26], J. Southward[26]; **Intensive Care Unit, Queen Margaret Hospital, Dunfermline** P. Allcoat[27], S. Gray[27], M. McDougall (Local Lead Investigator)[27]; **Intensive Care Unit, Raigmore Hospital, Inverness** J. Matheson[28], J. Whiteside (Local Lead Investigator)[28]; **Intensive Care Unit, Royal Alexandra Hospital, Paisley** D. Alcorn[29], K. Rooney (Local Lead Investigator)[29], R. Sundaram[29]; **Intensive Care Unit, Southern General Hospital, Glasgow** G. Imrie (Local Lead Investigator)[30]; **Intensive Care Unit, St John's Hospital, Livingston** J. Bruce[31], K. McGuigan[31], S. Moultrie (Local Lead Investigator)[31]; **Intensive Care Unit, Stirling Royal Infirmary** C. Cairns (Local Lead Investigator)[32], J. Grant[32], M. Hughes[32]; **Intensive Care Unit, Stobhill Hospital, Glasgow** C. Murdoch (Local Lead Investigator)[33]; **Intensive Care Unit, Victoria Hospital, Glasgow** A. Davidson (Local Lead Investigator)[34]; **Intensive Care Unit, Western General Hospital, Edinburgh** G. Harris[35], R. Paterson[35], C. Wallis (Local Lead Investigator)[35]; **Intensive Care Unit, Western Infirmary, Glasgow** S. Binning (Local Lead Investigator)[36], M. Pollock[36]; **Wellcome Trust Clinical Research Facility, Edinburgh** J. Antonelli[37], A. Duncan[37], J. Gibson[37], C. McCulloch[37], L. Murphy[37]; **Roslin Institute, University of Edinburgh** C. Haley[38], G. Faulkner[38], T. Freeman[38], D. A. Hume[38] & J. K. Baillie (Principal Investigator)[38].

[1]Benaroya Research Institute, 1201 9th Avenue, Seattle, Washington 98101-2795, USA. [2]West of Scotland Specialist Virology Centre, Gartnavel General Hospital, Glasgow and Clyde Health Board, 1053 Great Western Road, Glasgow G12 0YN, UK. [3]Health Protection Agency, Microbiology Services Colindale, 61 Colindale Avenue, London NW9 5EQ, UK. [4]Imperial College London, St Mary's Campus, Norfolk Place, London W2 1PG, UK. [5]Liverpool School of Tropical Medicine, Pembroke Place, Liverpool L3 5QA, UK. [6]National Institute for Medical Research (NIMR), The Ridgeway, London NW7 1AA, UK. [7]Roche, 340 Kingsland Street, Nutley, New Jersey 07110-1199, USA. [8]University College London, Gower Street, London, WC1E 6BT, UK. [9]The Roslin Institute and R(D)SVS, University of Edinburgh, Easter Bush, Midlothian EH25 9RG, UK. [10]Department of Women's and Children's Health, Institute of Translational Medicine, University of Liverpool, Alder Hey Children's Hospital, Liverpool L12 2AP, UK. [11]Epidemiology and Public Health, University of Nottingham, Clinical Sciences Building, City Hospital, Nottingham NG5 1PB, UK. [12]The Weatherall Institute of Molecular Medicine, University of Oxford, John Radcliffe Hospital, Oxford OX3 9DS, UK. [13]Wellcome Trust Sanger Institute, Wellcome Trust Genome Campus, Hinxton, Cambridge CB10 1SA, UK. [14]Department of Critical Care Medicine, The Queen's Medical Research Institute, College of Medicine and Veterinary Medicine, University of Edinburgh, 47 Little France Drive, Edinburgh EH16 4TJ, UK [15]Generation Scotland, University of Edinburgh, Molecular Medicine Centre, Western General Hospital, Crewe Road South, Edinburgh EH4 2XU, UK. [16]Intensive Care National Audit & Research Centre, Tavistock House, Tavistock Square, London WC1H 9HR, UK. [17]Intensive Care Unit, Aberdeen Royal Infirmary, Foresterhill, Aberdeen AB25 2ZN, UK. [18]Intensive Care Unit, Ayr Hospital, Dallmellington Road, Ayr KA6 6DX, UK. [19]Intensive Care Unit, Borders General Hospital, Melrose TD6 9BS, UK. [20]Intensive Care Unit, Crosshouse Hospital, Kilmarnock KA2 0BE, UK. [21]Intensive Care Unit, Dumfries and Galloway Royal Infirmary, Dumfries DG1 4AP, UK. [22]Intensive Care Unit, Glasgow Royal Infirmary, Glasgow G4 0SF, UK. [23]Intensive Care Unit, Hairmyres Hospital, Lanarkshire G75 8RG, UK. [24]Intensive Care Unit, Inverclyde Royal Hospital, Greenock PA16 0XN, UK. [25]Intensive Care Unit, Monklands Hospital, Airdrie ML6 0JS, UK. [26]Intensive Care Unit, Ninewells Hospital, Dundee DD1 9SY, UK. [27]Intensive Care Unit, Queen Margaret Hospital, Dunfermline KY12 0SU, UK. [28]Intensive Care Unit, Raigmore Hospital, Inverness IV2 3UJ, UK. [29]Intensive Care Unit, Royal Alexandra Hospital, Paisley PA2 9PN, UK. [30]Intensive Care Unit, Southern General Hospital, Glasgow G51 4TF, UK. [31]Intensive Care Unit, St John's Hospital, Livingston EH54 6PP, UK. [32]Intensive Care Unit, Stirling Royal Infirmary, Stirling FK8 2AU, UK. [33]Intensive Care Unit, Stobhill Hospital, Glasgow G21 3UW, UK. [34]Intensive Care Unit, Victoria Hospital, Glasgow G42 9TY, UK. [35]Intensive Care Unit, Western General Hospital, Crewe Road South, Edinburgh EH4 2XU, UK. [36]Intensive Care Unit, Western Infirmary, Glasgow G11 6NT, UK. [37]Wellcome Trust Clinical Research Facility, Western General Hospital, Crewe Road South, Edinburgh EH4 2XU, UK. [38]Division of Genetics and Genomics, The Roslin Institute, University of Edinburgh, Easter Bush, Midlothian EH25 9RG, UK.

METHODS

Mouse infection. Background-matched wild-type (>95% C57BL/6) and *Ifitm3*$^{-/-}$ mice[8] 8–10 weeks of age were maintained in accordance with UK Home Office regulations, UK Animals Scientific Procedures Act 1986 under the project licence PPL80/2099. This licence was reviewed by The Wellcome Trust Sanger Institute Ethical Review Committee. Groups of >5 isofluorane-anaesthetized mice of both genotype were intranasally inoculated with 10^4 p.f.u. of A/X-31 influenza in 50 µl of sterile PBS. In some experiments A/X-31 was substituted with 200 p.f.u. of A/England/195/09 influenza, or 50–10^3 p.f.u. of A/PR/8/34 (PR/8) or an otherwise isogenic virus with a deletion of the *NS1* gene (delNS1)[19], made as described[26]. Their weight was recorded daily and they were monitored for signs of illness. Mice exceeding 25% total weight loss were killed in accordance with UK Home Office guidelines. Littermate controls were used in all experiments.

Influenza virus quantification. Lungs from five mice per genotype were collected on days 1, 2, 3, 4 and 6 post-infection, weighed and homogenized in 5% weight/volume (w/v) of Leibovitz's L-15 medium (Invitrogen) containing antibiotic-antimycotic (Invitrogen). Samples were quantified for viral load by plaque assay in tenfold serial dilutions on Madin–Darby canine kidney (MDCK) cell monolayers overlaid with 1% Avicell medium[27]. Lungs were subjected to two freeze-thaw cycles before titration. Virus was also quantified by quantitative PCR with reverse transcription (qRT–PCR), wherein RNA was first extracted from lung, heart, brain and spleen using the RNeasy Mini Plus Kit (Qiagen). Purified RNA was normalized by mass and quantified with SYBR Green (Qiagen) using the manufacturer's instructions and 0.5 µM primers for influenza matrix 1 protein (*M1*) forward: 5′-TGA GTCTTCTAACCGAGGTC-3′, reverse: 5′-GGTCTTGTCTTTAGCCATTCC-3′ (Sigma-Aldrich) and mouse β-actin (*Actb*) forward: 5′-CTAAGGCCAACCGTG AAAAG-3′, reverse: 5′-ACCAGAGGCATACAGGGACA-3′. qPCR was performed on a StepOnePlus machine (Applied Biosystems) and analysed with StepOne software v2.1 (Applied Biosystems).

Western blotting. Lungs were homogenized in 5% w/v of Tissue Protein Extraction Reagent (Thermo Scientific) containing cOmplete Protease Inhibitor (Roche). Total protein was quantified by BCA assay (Thermo Scientific) and was normalized before loading into wells. Proteins were visualized with the following indicated primary antibodies: anti-mouse IFITM2 rabbit polyclonal was purchased from Santa Cruz Biotechnology (catalogue no. sc-66828); anti-Fragilis (Ifitm3) rabbit polyclonal antibody was from Abcam (catalogue no. ab15592). The IFITM3 and NΔ21 western blot using the A549 stable cell lines were probed with the anti-IFITM1 antibody from Prosci (catalogue no. 5807), which recognizes a conserved portion of the IFITM1, IFITM2 and IFITM3 proteins which is still present even in the absence of the first twenty one N-terminal amino acids. The LCL blots (including the A549 cell line lysate controls) were probed with either an antibody which is specific for the N terminus of IFITM3 (rabbit anti-IFITM3 (N-terminal amino acids 8–38) (Abgent, catalogue no. AP1153a)), or with anti-IFITM1 antibody from Prosci (catalogue no. 5807), as well as rabbit anti-MX1 (Proteintech, catalogue no. 13750-1-AP) and mouse anti-GAPDH (clone GAPDH-71.1) (Sigma, catalogue no. G8795). For the LCL immunoblots all antibodies were diluted in DPBS (Sigma) containing 0.1% Tween 20 (Sigma) and 5% non-fat dried milk (Carnation) and incubated overnight at 4 °C. All primary antibodies were consequently bound to the corresponding species-appropriate horseradish peroxidase-conjugated secondary antibodies (Dako). Actin antibody was purchased from either Abcam or Sigma, mouse monoclonal, catalogue no. A5316.

Pathological examination. 5-µm sections of paraffin-embedded tissue were stained with haematoxylin and eosin (Sigma-Aldrich) and were examined and scored twice, once by a pathologist under blinded conditions. The TUNEL assay for apoptosis was conducted using the TACS XL DAB *In Situ* Apoptosis Detection Kit (R&D Systems).

Immunofluorescent tissue staining: protein. Lung tissue was embedded in glycol methacrylate (GMA) to visualize the spread of viral protein, as described previously[28]. Briefly, 2-µm sections were blocked with 0.1% sodium azide and 30% hydrogen peroxide followed by a second block of RPMI 1640 (Invitrogen) containing 10% fetal calf serum (Sigma-Aldrich) and 1% bovine serum albumin (Invitrogen). Viral antigen was stained using M149 polyclonal antibody to influenza A, B (Takara) and visualized with a secondary goat anti-rabbit antibody conjugated to alkaline phosphatase (Dako). Sections were counterstained with haematoxylin (Sigma-Aldrich). Murine IFITM1 and IFITM3 protein expression in lung sections from either uninfected mice, or those 2 days post-infection with A/X-31, were immunostained with either anti-IFITM1 antibody (Abcam, catalogue no. ab106265) or anti-fragilis (anti-Ifitm3) rabbit polyclonal antisera (Abcam, catalogue no. ab15592). Sections were also stained for DNA with Hoechst 33342 (Sigma).

Immunofluorescent staining: RNA. Viral RNA was visualized in 5-µm paraffin-embedded sections using the QuantiGene viewRNA kit (Affymetrix). Briefly, sections were rehydrated and incubated with proteinase K. They were subsequently incubated with a viewRNA probe set designed against the negative stranded viral RNA encoding the *NP* gene of A/X-31 (Affymetrix). The signal was amplified before incubation with labelled probes and visualized.

Flow cytometry. Single-cell suspensions were generated by passing lungs twice through a 100-µm filter before lysing red blood cells with RBC lysis buffer (eBioscience) and assessing for cell viability via Trypan blue exclusion. Cells were characterized by flow cytometry as follows: T-lymphocytes $CD4^+$ or $CD8^+$, T-lymphocytes (activated) $CD4^+CD69^+$ or $CD8^+CD69^+$, neutrophils $CD11b^{hi}CD11c^-Ly6g^+$, dendritic cells $CD11c^+CD11b^{lo}Ly6g^{lo}$ MHC class II high, macrophages $CD11b^+CD11c^+F4/80^{hi}$, natural killer cells $NKp46^+CD4^-CD8^-$. All antibodies (Supplementary Table 3) were from BD Bioscience, except CD69 and F4/80, which were from AbD Serotec. Samples were run on a FACSAria II (BD Bioscience) and visualized using FlowJo 7.2.4. Data were analysed statistically and graphed using Prism 5.0 (GraphPad Software).

Peripheral leukocyte analysis. Mice ($n = 3$ per genotype per day) were bled on days 0, 1, 2, 3, 4 and 6 by tail vein puncture. Leukocyte counts were determined by haemocytometer, whereas blood cell differential counts were calculated by counting from duplicate blood smears stained with Wright–Giemsa stain (Sigma-Aldrich). At least 100 leukocytes were counted per smear. All blood analyses were conducted in a blinded fashion. Data were analysed statistically and graphed using Prism 5.0 (GraphPad Software).

Cytokine/chemokine analysis. Lungs were collected and homogenized on days 0, 1, 2, 3, 4 and 6 post-infection from four mice of each genotype. G-CSF, GM-CSF, IFN-γ, IL-10, IL-1α, IL-1β, IL-2, IL-4, IL-5, IL-6, IL-9, IP-10, KC-like, MCP-1, MIP-1α, RANTES and TNF-α were analysed using a mouse antibody bead kit (Millipore) according to the manufacturer's instructions on a Luminex FlexMAP3D. Results were analysed and quality control checked using Masterplex QT 2010 and Masterplex Readerfit 2010 (MiraiBio). Data were analysed statistically and graphed using Prism 5.0 (GraphPad Software).

Murine embryonic fibroblast generation, transduction and infectivity assays. Adult *Ifitm3*$^{-/-}$ mice[8] were intercrossed and fibroblasts (MEFs) were derived from embryos at day 13.5 of gestation, as described previously[1]. MEFs were genotyped by PCR (Thermo-Start *Taq* DNA Polymerase, ABgene) on embryo tail genomic DNA using primers and the cycle profile described previously[8] to detect the presence of the wild-type allele (450 base pairs band) and the targeted/knock-out allele (650 bp band). MEFs were cultured in DMEM containing 10% FBS, 1× MEM essential amino acids, 1× 2-mercapto-ethanol (Gibco). MEFs were transduced with vesicular stomatitis virus G (VSV-G) pseudotyped retroviruses expressing either the empty vector control (pQXCIP, Clontech), or one expressing *Ifitm3*, as previous described[1]. After puromycin selection the respective cell lines were challenged with either A/X-31 virus (multiplicity of infection (m.o.i.) 0.3–0.4) or PR/8 (m.o.i. 0.4). For PR/8 infections, after 12 h the media was removed and the cells were then fixed with 4% formalin and stained with purified anti-haemagglutinin monoclonal antibody (Hybridoma HA36-4-5.2, Wistar Institute). For A/X-31 experiments, cells were processed comparably as above, but in addition were permeabilized, followed by immunostaining for NP expression (NP (clone H16-L10-4R5) mouse monoclonal (Millipore MAB8800)). Both sets of experiments were completed using an Alexa Fluor 488 goat anti-mouse secondary antibody at 1:1,000 (A11001, Invitrogen). The cells were imaged on an automated Image Express Micro microscope (Molecular Devices), and images were analysed using the MetaMorph Cell Scoring software program (Molecular Devices). Cytokines: cells were incubated with cytokines for 24 h before viral infection. Murine interferon α (PBL Interferon Source, catalogue no. 12100-1) and IFN-γ (PBL Interferon Source, catalogue no. 12500-2) were used at 500–2,500 U ml^{-1}, and 100–300 ng ml^{-1}, respectively.

A549 transduction and infectivity assays. A549 cells (ATCC catalogue no. CCL-185) were grown in complete media (DMEM (Invitrogen catalogue no. 11965) with 10% FBS (Invitrogen)). A549 stable cell lines were made by gamma-retroviral transduction using either the empty vector control virus (pQXCIP, Clontech), the full-length human *IFITM3* complementary DNA, or a truncated human *IFITM3* cDNA which is missing the first 21 amino acids (NΔ21). After puromycin selection, expression of the IFITM3 and NΔ21 proteins were confirmed by western blotting using an 18% SDS–PAGE gel and an anti-IFITM3 antibody that was raised against the conserved intracellular loop (CIL) of IFITM3 (Proteintech). A549 cell lines were challenged with one of the following strains: A/WSN/33 (a gift of P. Palese), A/California/7/2009, A/Uruguay/716/2007 and B/Brisbane/60/2008 (gift of J. Malbry) for 12 h, then fixed with 4% paraformaldehyde (PFA) and immunostained with anti-HA antibody (Wistar collection) or anti-NP antibodies (Abcam), or Millipore clone H16-L10-4R5 anti-influenza A virus antibody). Per cent infection was calculated from immunofluorescent images as described for the MEF experiments above. Alternatively, cells were transduced with lentiviral vectors to express green fluorescent protein (GFP) or IFITM3 and were stained with anti-NP antibody (Abcam) and analysed by flow cytometry following

challenge with B/Bangladesh/3333/2007 virus (NIMR, England). For the immunofluorescence-based viral titring experiments, virus-containing supernatant was collected from the indicated A549 cell line cultures after 12 h of infection with WSN/33 (part one). Next this supernatant was used to infect MDCK cells (ATCC) in a well by well manner (part two). Both the A549 and MDCK cells were then processed to detect viral HA expression as described above.

LCL infectivity assays. LCL TT and LCL CC cells were grown in RPMI-1640 (Sigma-Aldrich) containing 10% FCS, 2 mM L-glutamine, 1 mM sodium pyruvate, 1× MEM non-essential amino acids solution, and 20 mM HEPES (all from Invitrogen). For infectivity assays, LCL cells were either treated with recombinant human IFN-α2 (PBL Interferon Source, catalogue no. 11100) at 100 units per ml or DPBS (Sigma-Aldrich) for 16 h. The LCL cells were then counted, resuspended at a concentration of 5×10^5 cells per ml, and plated on a 96-well round-bottom plate (200 µl cell suspension per well). The cells were then challenged with WSN/33 influenza A virus (m.o.i. 0.1). After 18 h, the cells were washed twice with 250 µl MACS buffer (DPBS containing 2% FCS and 2 mM EDTA (Sigma-Aldrich)). The cells were fixed and permeabilized using the BD Cytofix/Cytoperm Fixation/Permeabilization Kit (BD Biosciences), following the manufacturer's instructions. Briefly, the cells were resuspended in 100 µl of Cytofix/Cytoperm Fixation and Permeabilization solution and incubated at 4 °C for 20 min. The cells were then washed twice with 250 µl 1× Perm/Wash buffer and resuspended in 50 ml 1× Perm/Wash buffer containing a 2 µg ml^{-1} solution of a fluorescein isothiocyanate (FITC)-conjugated mouse monoclonal antibody against influenza A virus NP (clone 431, Abcam, catalogue no. ab20921). The cells were incubated in the diluted antibody solution for 1 h at 4 °C, washed twice with 250 µl 1× Perm/Wash buffer, resuspended in 200 µl MACS buffer, and analysed by flow cytometry using a BD FACS Calibur (BD Biosciences).

Ethics and sampling. We recruited patients with confirmed seasonal influenza A or B virus or pandemic influenza A pH1N1/09 infection who required hospitalization in England and Scotland between November 2009 and February 2011. Patients with significant risk factors for severe disease and patients whose daily activity was limited by co-morbid illness were excluded. 53 patients, 29 male and 24 female, average age 37 (range 2–62) were selected. 46 (88%) had no concurrent co-morbidities. The remaining 6 had the following comorbid conditions: hypertension (3 patients), alcohol dependency and cerebrovascular disease (1 patient), bipolar disorder (1 patient) and kyphoscoliosis (1 patient). Four patients were pregnant. Where assessed, 36 patients had normal body mass (69%), one had a body mass index <18.5 and 10 had a body mass index between 25 and 39.9 and one a body mass index >40. Seasonal influenza A H3N2, influenza B and pandemic influenza A pH1N1/09 were confirmed locally by viral PCR or serological tests according to regional protocols. Consistent with the prevalent influenza viruses circulating in the UK between 2009 and 2011 (ref. 29) 44 (85%) had pH1N1/09, 2 had pH1N1/09 and influenza B co-infection, 4 had influenza B and 2 had non-subtyped influenza A virus infection. Of the adults, 24 required admission to an intensive care unit (ICU) and 1 required admission to a high dependency unit (HDU). The remainder were managed on medical wards and survived their illnesses. The GenISIS study was approved by the Scotland 'A' Research Ethics Committee (09/MRE00/77) and the MOSAIC study was approved by the NHS National Research Ethics Service, Outer West London REC (09/H0709/52, 09/MRE00/67).

Consent was obtained directly from competent patients, and from relatives/friends/welfare attorneys of incapacitated patients. Anonymized 9-ml EDTA blood samples were transported at ambient temperature. DNA was extracted using a Nucleon Kit (GenProbe) with the BACC3 protocol. DNA samples were re-suspended in 1 ml TE buffer pH 7.5 (10 mM Tris-Cl pH 7.5, 1 mM EDTA pH 8.0).

Sequencing and genetics. Human *IFITM3* sequences were amplified from DNA obtained from peripheral blood by nested PCR (GenBank accession numbers JQ610570 to JQ610621). The first round used primers forward: 5′-TGAGGGT TATGGGAGACGGGGT-3′and reverse: 5′-TGCTCACGGCAGGAGGCC-3′, followed by an additional round using primers forward: 5′-GCTTTGGGGGA ACGGTTGTG-3′and reverse: 5′- TGCTCACGGCAGGAGGCCCGA-3′. The 1.8-kb *IFITM3* band was gel-extracted and purified using the QIAquick Gel Extraction Kit (Qiagen). *IFITM3* was Sanger-sequenced on an Applied Biosystems 3730xl DNA Analyzer (GATC Biotech) using a combination of eight sequencing primers (Supplementary Table 4). Single-nucleotide polymorphisms were identified by assembly to the human *IFITM3* encoding reference sequence (accession number NC_000011.9) using Lasergene (DNAStar). Homozygotes were called based on high, single base peaks with high Phred quality scores, whereas heterozygotes were identified based on low, overlapping peaks of two bases with lower Phred quality scores relative to surrounding base calls (Supplementary Fig. 9). We identified SNP rs12252 in our sequencing and compared the allele and genotype frequencies to allele and genotype frequencies from 1000 Genomes sequencing data from different populations (Supplementary Table 3). In addition, we used the most recent release of phased 1000 Genomes data[30] to impute the region surrounding SNP rs12252 to determine allele frequencies in the publicly available genotype data set of WTCCC1 controls ($n = 2{,}938$) and four previously published data sets genotyped from the Netherlands ($n = 8{,}892$) and Germany ($n = 6{,}253$)[22]. In the imputation, samples genotyped with Illumina 550k, 610k and 670k platforms were imputed against the June 2011 release of 1000 Genotypes phased haplotypes using the Impute software[31], version 2.1.2. Only individuals with European ethnicities (Europe (CEU), Finland (FIN), Great Britain (GBR), Spain/Iberia (IBS), Tuscany (TSI)) were included from the 1000 Genomes reference panel. Recommended settings were used for imputing the region 200 kb in either direction from the variants of interest, along with 1 Mb buffer size. The statistical significance of the allele frequencies was determined by Fisher's exact test.

We assessed for population stratification by principal component analysis. Genotype data from the WTCCC1 1958 Birth Cohort data set were obtained from the European Genotype Archive with permission, reformatted and merged with genotype data from the GenISIS study to match 113,819 SNPs present in both cohorts. Suspected strand mismatches were removed by identifying SNPs with more than 2 genotypes and using the LD method as implemented in Plink (v1.07)[32], resulting in 105,362 matched SNPs. Quality control was applied in GenABEL version 1.6-9 to genotype data for these SNPs for the GenISIS cases and 1,499 individuals from WTCCC. Thresholds for quality control (deviation from Hardy–Weinberg equilibrium ($P < 0.05$), minor allele frequency (MAF) < 0.0005, call rate <98% in all samples) were applied iteratively to identify all markers and subjects passing all quality control criteria, followed by principal component analysis using GenABEL. We tested for positive selection using both a haplotype-based test (|XP-EHH-max|) and allele frequency spectrum-based test statistics, namely the CLR[23–25] on 10-kb windows across the entire genome as described previously[30,33]. The three statistics were combined and the combined *P* value was plotted corresponding to the 10-kb windows.

26. de Wit, E. *et al.* Efficient generation and growth of influenza virus A/PR/8/34 from eight cDNA fragments. *Virus Res.* **103,** 155–161 (2004).
27. Hutchinson, E. C., Curran, M. D., Read, E. K., Gog, J. R. & Digard, P. Mutational analysis of *cis*-acting RNA signals in segment 7 of influenza A virus. *J. Virol.* **82,** 11869–11879 (2008).
28. Britten, K. M., Howarth, P. H. & Roche, W. R. Immunohistochemistry on resin sections: a comparison of resin embedding techniques for small mucosal biopsies. *Biotech. Histochem.* **68,** 271–280 (1993).
29. Ellis, J. *et al.* Virological analysis of fatal influenza cases in the United Kingdom during the early wave of influenza in winter 2010/11. *Eurosurveillance* **16,** 2–7 (2011).
30. The 1000 Genomes project Consortium. A map of human genome variation from population-scale sequencing. *Nature* **467,** 1061–1073 (2010).
31. Howie, B. N., Donnelly, P. & Marchini, J. A flexible and accurate genotype imputation method for the next generation of genome-wide association studies. *PLoS Genet.* **5,** e1000529 (2009).
32. Purcell, S. *et al.* PLINK: a toolset for whole-genome association and population-based linkage analysis. *Am. J. Hum. Genet.* **81,** 559–575 (2007).
33. MacArthur, D. G. *et al.* A systematic survey of loss-of-function variants in human protein-coding genes. *Science* **335,** 823–828 (2012).